Shear stiffness and energy absorption of auxetic open cell foams as sandwich cores

Hong Chun Cheng[1], Fabrizio Scarpa[1,2]*, Tulio Hallak Panzera[2,3], Ian Farrow[1,2], Hua-Xin Peng[4]

[1]Aerospace Engineering, CAME, University of Bristol, BS8 1TR Bristol, UK

[2]Bristol Composites Institute (ACCIS), University of Bristol, BS8 1TR Bristol, UK

*Corresponding Author: f.scarpa@bristol.ac.uk

[2]Centre for Innovation and Technology in Composite Materials (CIT^{e}C), Department of Mechanical Engineering, Federal University of São João del Rei - UFSJ, Brazil.

[4]Institute for Composites Science Innovation (InCSI), School of Materials Science and Engineering, Zhejiang University, Hangzhou 310027, PR China

Abstract. *This work describes the identification of the shear modulus of open cell polyurethane thermoformed auxetic foams from 3-point and 4-point bending tests. The foams are incorporated in sandwich beams with carbon fibre/epoxy face skins, and benchmarked against similar sandwich structures made with the conventional counterpart open cell foam. Three types of beams are tested: one with auxetic foams, another type related to a conventional foam core with the same thickness of the auxetic porous materials, and a third type of beam consisting in conventional foam with a thickness corresponding to an iso-weight configuration to the auxetic specimen. The auxetic foam has a shear modulus 7% lower than the one of the bulk conventional specimens, but higher shear stresses at large deformations and a smoother strain stiffening response compared to the beams with the conventional thinner core. The paper also highlights the low shear wave speed of these auxetic foams compared to other porous polymers used in helmet and head protection applications, as well as potential uses of the quasi-zero-stiffness behaviour here observed for the auxetic foam sandwich beam.*

Keywords: auxetic, foam, shear, bending, experiments, energy absorption.

1. Introduction

More than 30 years ago the seminal Science paper of Roderic Lakes instilled the interest of manufacturing negative Poisson's ratio (NPR) foams [1]. Although systems with auxetic [2] characteristics have been proposed and evaluated before by other Authors [3][4][6] with further developments [5][7][8], the production of open cell foams exhibiting NPR has been probably one of the first and most successful manufacturing outputs in auxetic systems. Auxetic (NPR) foams have demonstrated a large number of beneficial properties for practical applications, like increased indentation resistance, shear stiffness, plane strain fracture toughness, enhanced acoustic properties and the ability to form sinclastic curvature [9]. The production of auxetic foams can be performed using several techniques, from thermoforming [10][11][12], chemical solvent [13][14] and carbon dioxide-assisted compression methods [15]. Foams produced using these techniques have been extensively tested for compressive and fatigue cycling [16], vibration damping [17], and a variety of protective liners for sports and helmet applications [18][19][20].

One aspect that is somehow overlooked in open literature is the behaviour of auxetic foams under shear. Zhu *et al* have provided estimates of the shear modulus in conventional foams with tetrakaidekahedral cells [21]. Andersson *et al* have estimated the shear modulus of flexible polyurethane foams by using compressive and creep tests with dynamic mechanical analysers [22]. A more comprehensive set of data encompassing both the compressive modulus and the shear one obtained from torsion tests on a series of rigid open cell PU foams has been presented by Thompson *et al* [23]. To the best of the Authors' knowledge, no direct experimental measurement of the shear modulus in auxetic foams has appeared so far in open literature. This work aims at filling this specific gap, in particular by focusing on the properties of an auxetic open cell PU foam produced following the process outlined in [11]. The shear modulus is extracted here from 3-point and 4-point bending tests on sandwich panels made from auxetic core and carbon fibre/epoxy unidirectional face skins. The tests are carried out following the corresponding ASTM standard [24]. To cater for the increased density of auxetic foam compared to their conventional counterpart, we have here prepared sandwich beam samples with conventional foam having the same weight, or equal core thickness of the auxetic specimens. The results will show that the auxetic foams have a significantly lower shear modulus compared to the conventional ones from which they are derived. The sandwich beams

made with the negative Poisson's ratio foam do exhibit a shear stress stiffening at large deformations, opposite to the specimen with the conventional cores. Moreover, the auxetic core beams feature a quasi-zero stiffness behaviour at large bending deformations, and a smooth softening response which differs from the negative stiffness one provided by the beams with the conventional core and similar thickness.

The paper also contains a series of discussions about the benchmarking and potential use of these auxetic foams for applications ranging from helmet to vibration impact absorbers. The discussions are corroborated by the data shown in this work, and design guidelines/considerations from open literature.

2. Manufacturing and testing

The sandwich beam specimens have been designed and produced following the dimensions recommended by the ASTM D7250/D7250M [24]. The dimensions of the conventional foam core for the reference sandwich panels are 200 mm × 80 × 35 mm. Three types of foams are considered as core material (Table 1): (i) auxetic foam, (ii) conventional foam (thin) with similar thickness and (iii) conventional foam (thick) with similar mass. The open cell polyurethane foam was HR70 and supplied by Cardiff Upholstery Ltd (30 pores per inch). The nominal density of the foam is 27 kg m^{-3}, but in-house measurements carried out on 15 samples prior to assembly gives a value of 30±1.8 kg m^{-3}. A conventional foam sheet with the same nominal 35 mm thickness is used to produce the auxetic foams. The foam sheet is placed on an aluminium mould, vacuum-bagged and thermoformed following the procedure outlined in [11]. The foam sheet is trimmed at the margins to obtain homogeneous plates of 200 mm × 80 mm sides. The weight of the conventional thick core foam samples is 4.50 ±0.8 g. The Auxetic foam blocks have a weight of 4.43±1.1 g, with a 1.5% difference compared to the conventional porous slabs. The equivalent density of the auxetic foam is 188 ±9 kg m^{-3}, 6.26 times higher than the conventional foam.

Table 1. Thickness and mass of the sandwich beams.

Foam type	Thickness (mm)	Mass (g)
i. Auxetic	9.16 ± 0.53	24.95 ± 0.18
ii. Conventional Thin	10.59 ± 0.11	14.12 ± 0.29
iii. Conventional Thick	36.24 ± 0.11	26.51 ± 0.21

Sandwich panels are made using Hexcel IM7/8852 carbon/epoxy prepregs as skins [25] (one layer, 0.125 mm). Prepregs are used as unidirectional skins (0^o) with the fibre direction parallel to the length of the core. The single laminae are initially cured at approximately 120 ^{o}C for 120 min following the NMS 128/2 manufacture guidelines. The cured prepregs are then cold-bonded to the foam cores using a commercial epoxy polymer adhesive (Araldite AB) with 2:1 mix ratio. Five samples are manufactured for each core type (Figure 1). A flat metal plate of constant mass (2kg) is placed upon each panel to ensure a minimum contact pressure during the curing time of 24h at room temperature. The thickness and mass of the sandwich beams are reported in Table 1.

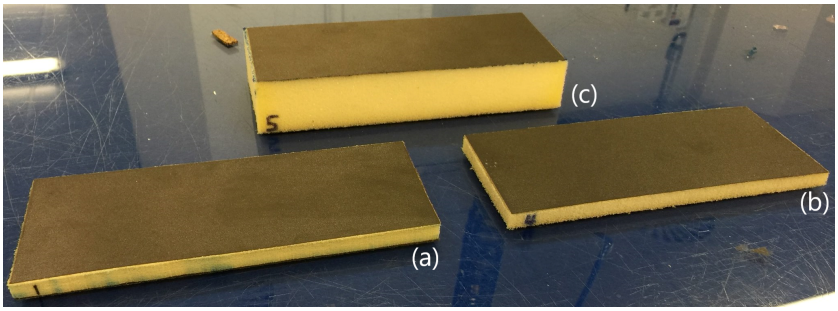

Fig. 1. Sandwich panels made with: auxetic (a), conventional thin (b) and conventional thick (c) foam cores.

Tensile tests on conventional and auxetic foam strips (thickness ~ 9 mm) are carried out to obtain the in-plane Poisson's ratio. The tests are performed using a 1 kN Instron 3343 (3343K8827) testing machine, with position accuracy of 0.5% (±10μm) and load accuracy of 0.5% (±0.1 N). The tests are carried out at a crosshead rate of 1 mm/min. The Poisson's ratio is obtained using an Imetrum video gauge system to measure the strain fields along the loading and the transverse directions related to the central portion (50%) of the samples (see Figure 2a). Fiducial markers have been used to measure the deformations and obtain equivalent strains [11]. In this case, the definition of Poisson's ratio used is the classical one ($\nu_{xy} = -\varepsilon_y/\varepsilon_x$).

The same universal testing machine is used to perform 3-point and 4-point bending tests using support span lengths of 150 mm. For 4-point test, the loading span (L) is chosen as 50 mm, which is one-third of the support span length according to the ASTM D7250/D7250M. The dimensions of the beams are the same for the two different types of tests (length 200 mm, width 80 mm). Tests are conducted under single loading (30 mm of maximum deflection), and cyclic loading (10 and 30 mm of maximum deflection for the 3P and 4P bending tests, respectively) with a cross-head rate at 2 mm/min. The tests are used to obtain the core shear

modulus (G_C) and panel flexural stiffness according to the formulas provided in the ASTM standard [24]. The shear strain is calculated for the 3P and 4P bending tests as follows [26]:

$$\gamma_c = \frac{F}{2bdG_c} \tag{1}$$

In (1), F is the central force, b and d are the width and thickness of the beams, respectively. The core shear stress, which is used for the 3-point bending specimens, and also for the 4-point tests as reference is [26]:

$$\tau_c = \frac{F}{2bd} \tag{2}$$

The loss factor under cyclic loading is evaluated as:

$$\eta = \frac{\Delta W}{2\pi W} \tag{3}$$

In Eq. (3) ΔW is the energy dissipated during the cycle, while W is the work produced on the foam sample under the loading phase. The term 2π is used to because the loading/unloading displacement is harmonic. All tests are carried out at room temperature (19 ^oC). There was no specific control of the humidity, although the average RH during the tests was 15%.

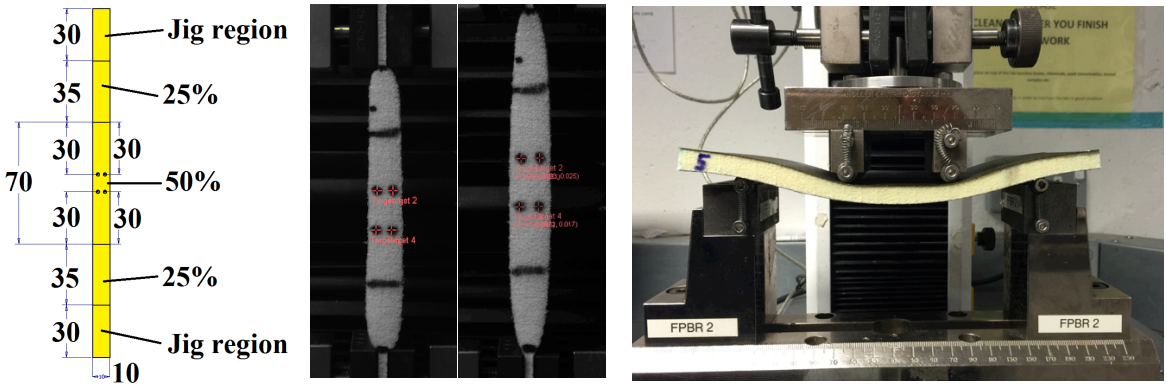

(a) **(b)**

Fig. 2 (a) Layout for Poisson's ratio measurement and evidence of NPR in the foams produced, (b) 4-point bending rig with an auxetic foam core sandwich being tested.

3. Results

3.1 Poisson's ratio of the core foams

Figure 3 shows the variation of the Poisson's ratio against the tensile strain for the two types of foam specimens. The auxetic foam shows a clear NPR, with a Poisson's ratio of -1.33 observed for a maximum strain of 17.9%. Because of the manufacturing process used in this work [11], the foam produced is likely to be anisotropic. Moreover, these results are consisted with other thermoformed auxetic foams presented in open literature [11]. The average Poisson's ratio value for the conventional PU foam is positive and equal to 0.39. Also, this value is consistent with other observations from open literature [16] [22].

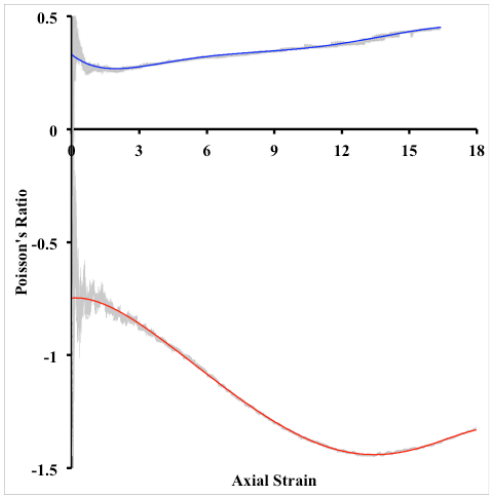

Fig. 3. In-plane Poisson's ratios of the conventional (top, blue) and auxetic (bottom, red) foams. Axial strain is in percentage. The red and blue lines are fit for the experimental data.

3.2 Core shear modulus and panel flexural stiffness

Figure 4 shows the values for the core shear modulus, panel transverse shear rigidity (via 3-P and 4-P bending tests) and panel flexural stiffness (via 3-P bending test). The values of the shear modulus of the conventional foam found through the bending tests are consistent with the ones from torsion and creep tests in PU open foams with similar densities [22][23]. As a verification, by taking the Young's modulus of the conventional foam measured here equal to 130 kPa [27] and the Poisson's ratio of 0.39 (Figure 3), a shear modulus of 47 kPa is obtained

based on Hookes´s law for an isotropic material ($G = E/2(1+\nu)$), which is in a very good agreement with the results found through the bending test (thick samples).

A higher core shear modulus is observed in panels made with the conventional thin foam. Other values in descending order are provided by the thick conventional, and finally by the auxetic one (Figure 4a). The value of the core conventional shear modulus appears slightly reduced when extracted from the 4-point bending tests. An opposite behaviour is however observed for the auxetic panels, with its value increasing almost by 25% between the 3-P to 4-P tests. The 4-point test generates a pure constant bending moment and zero shear across the supports, which increases the effect of the core compression [26], and therefore contributes to the stiffening of the auxetic foam along the transverse direction (Figure 4a). The transverse shear rigidity is – as expected - significantly affected by the core thickness, with its highest values corresponding to the conventional thick foam samples. The auxetic panels show a 24% increase in transverse shear rigidity when characterised using the 4-P bending tests (Figure 4b). Also in this case, this behaviour can be explained by the stiffening NPR effect under transverse loading. Figure 4c shows the very remarkable (and expected) increase in flexural stiffness (~12 times in logarithmic scale) achieved by the panels made with the conventional thick foam core. Panels fabricated with conventional thin foam presented a logarithmic increase of 32% in flexural stiffness when compared to auxetic ones.

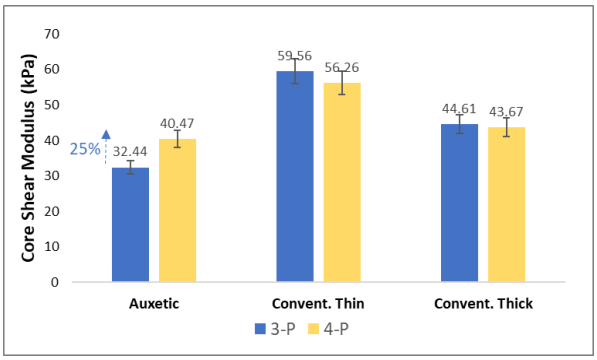

(a)

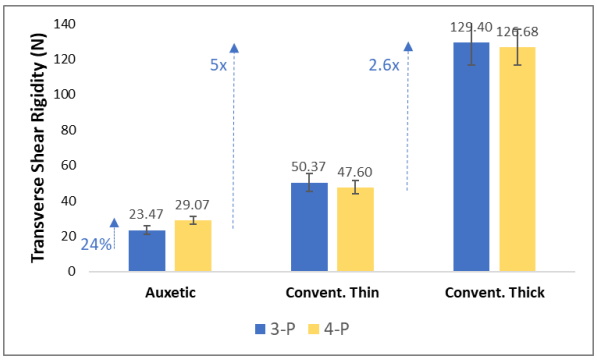

(b)

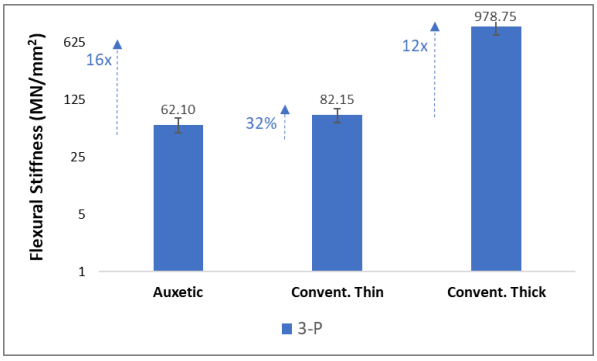

(c)

Fig. 4. Core shear modulus (a), panel transverse shear rigidity (b) and panel flexural stiffness(c). Blue indicates 3P bending, while grey relates to 4P. Five samples for each configuration are tested.

Figure 5 shows the mechanical behaviour of the panels under 3P (a) and 4P (b) bending tests. After approximately 20 mm of displacement, the auxetic panel tend to show a greater stiffness compared to the conventional thin ones. The conventional thin panels have also a clear negative stiffness behaviour in bending, both under 3P and 4P loading. The thick conventional foam sandwich panels show a more monotonic and stiffer response under 4P [26]. The thin sandwich samples also show a similar stiffening effect, although the postbuckling behaviour of the thin conventional panel is less abrupt. The auxetic panel reveals instead a common path of softening, but always maintaining a positive tangent stiffness, veering almost to a quasi-zero one at larger extensions (Figure 5b).

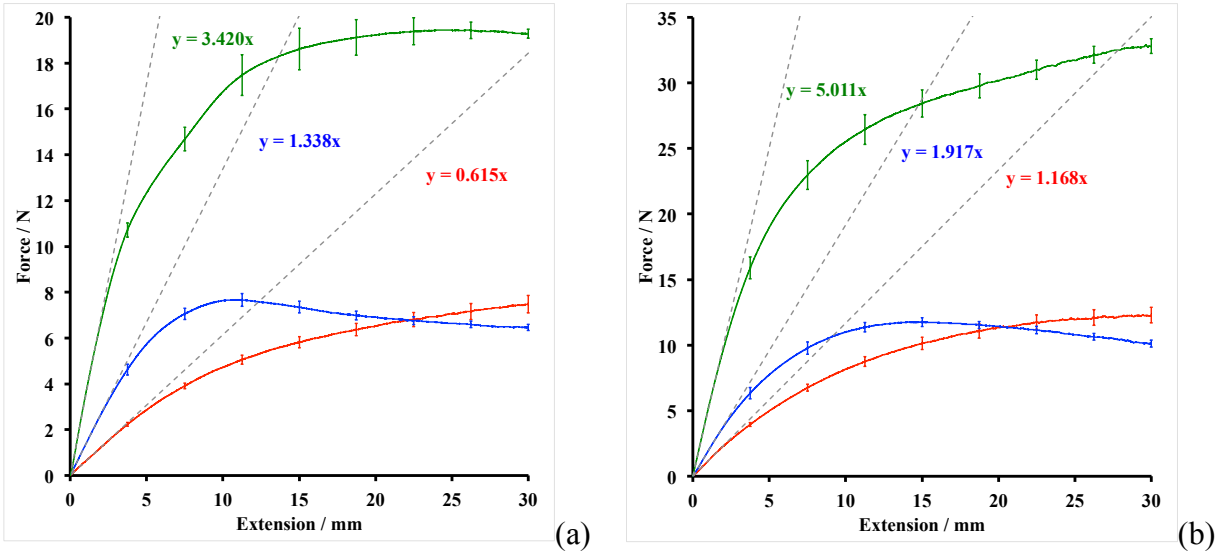

(a) (b)

Fig. 5. Force vs. central deflection for (a) 3-point and (b) 4-point bending. Red: auxetic, blue: conventional thin, green: conventional thick. Note the quasi-zero stiffness behaviour of the auxetic beam at large extensions

Figures 6a and 6b show the normalised (specific) flexural behaviours under 3P and 4P loading, respectively. The central deflections are also normalised versus the beam spans; these are the strains contained in the Figures. Also in these cases, the largest specific force per unit weight is provided by the conventional thick panel, followed by the conventional thin and

auxetic ones. At the maximum strain the ratios between the specific forces is 12.1:7.5:4.2. At small strain little difference is observed in terms of specific stiffness between the panels with the conventional foams. Both under 3P and 4P bending, the auxetic sandwich panel is however 2.4 times less stiff than the analogous thin conventional one at small strains (0.025).

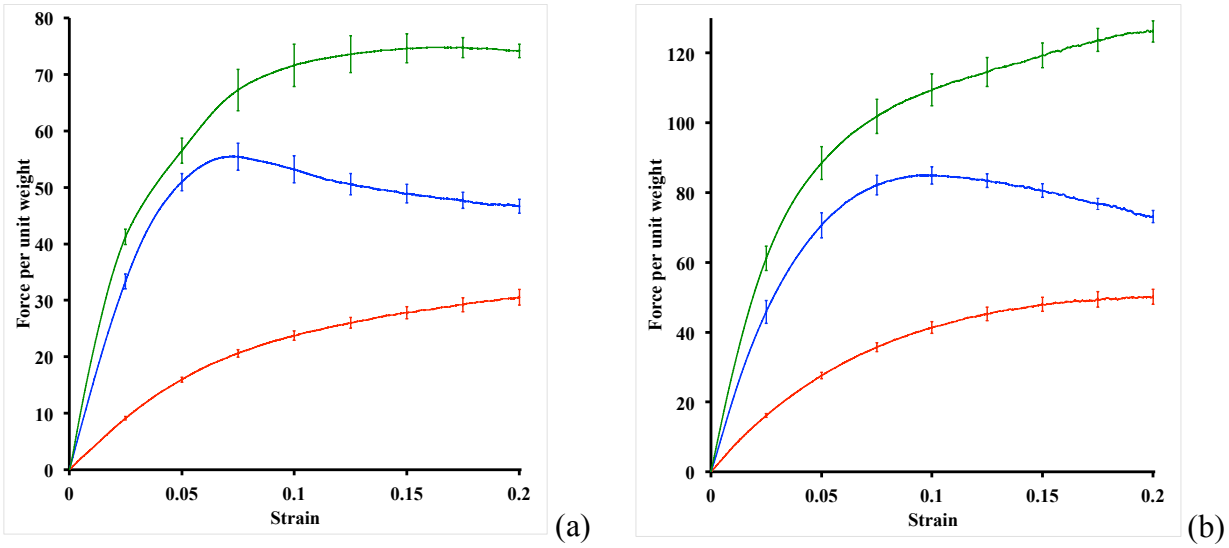

Fig. 6. Normalised force (N/N) vs. strain for (a) 3-point and (b) 4-point bending. Red: auxetic, blue: conventional thin, green: conventional thick.

Figures 7 the behaviour under 3P and 4P bending of the core shear stress (Equation 2) versus the shear strain (Equation 1). The linear interpolations are used to calculate the shear modulus for each type of sandwich beam. From a qualitative point of view, these curves follow similar trends to the ones observed in Figures 5 and 6, with parallel considerations regarding the difference between 3P and 4P loading. It is however very interesting to note that at larger shear strains (> 20% for 3P and 30% for 4P) the auxetic core beams provide a larger shear stress than the conventional panels, with up to 25% higher core shear stress at a shear strain 0f 60% (Figure 7b). It is worth noticing that at larger shear strains the beams with the conventional cores tend to asymptotically approach the same shear stiffness, in particular for the 4P bending case.

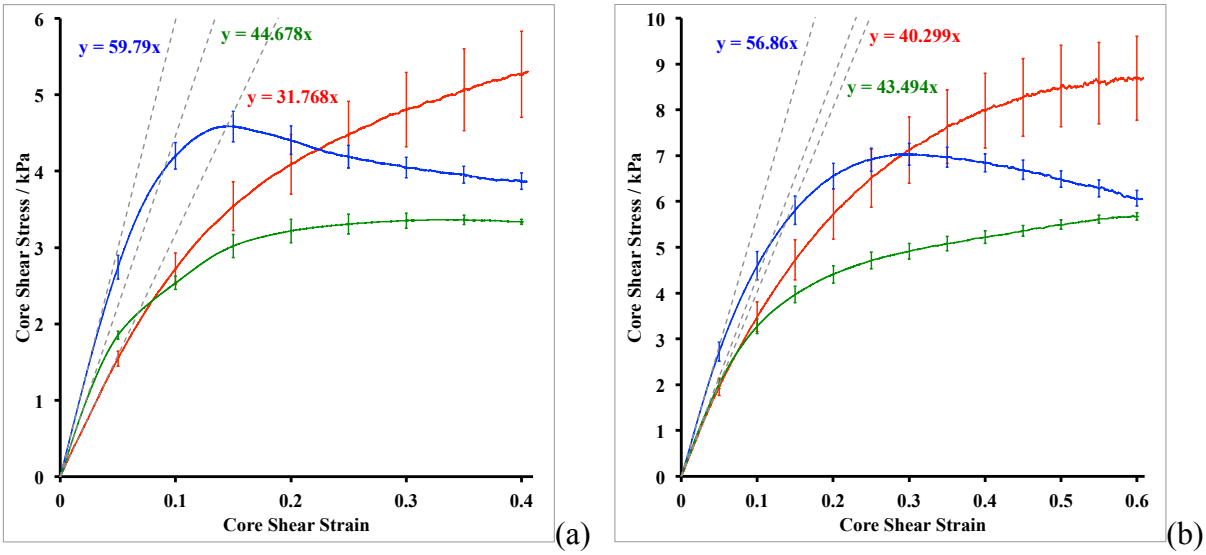

Fig. 7. Core shear stress against core shear strain under 3-point (a) and (b) 4-point direct test. Red: auxetic, blue: conventional thin, green: conventional thick.

3.3 Energy absorption and loss factors

Figure 8 shows the average of the hysteresis curves for panels tested under 3P (a) and 4P (b) point bending for a maximum central deflection of 10 mm. Table 2 presents the dissipated energies and loss factors calculated from Equation 3 for the same maximum central deflections.

Table 2. Energy dissipated and loss factor for the 3-P and 4-P tests (10 mm deflections)

Property	Test	**Auxetic**	**Conventional Thin**	**Convention Thick**
Energy dissipated (J)	**3-P**	8.2 ± 3.3	16.4 ± 8.5	34.5 ± 6.8
	4-P	16.9 ± 12.3	24.5 ± 11.0	56.6 ± 12.0
Loss factor [%]	**3-P**	4.68 ± 0.22	5.06 ± 0.11	4.72 ± 0.22
	4-P	5.35 ± 0.35	5.74 ± 0.15	5.09 ± 0.14

The shape of the hysteresis curves is quite similar for all the three foam cases considered, although it is possible to observe more clearly in the conventional foams some of the postbuckling behaviours discussed in section 3.2.

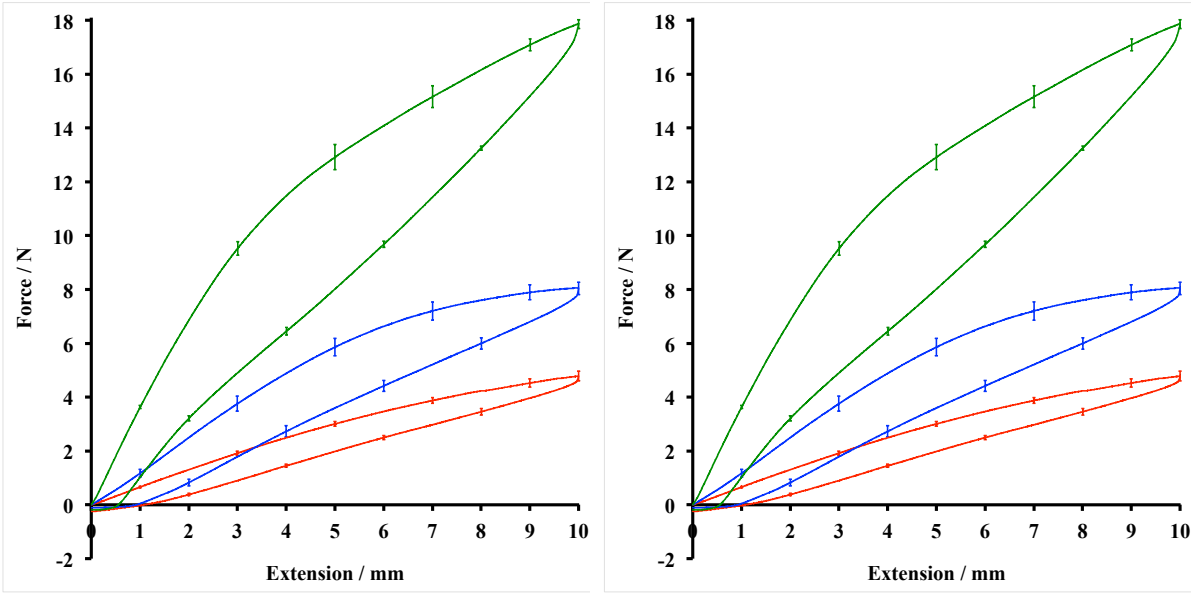

(a) **(b)**

Fig. 8. Hysteresis curves for (a) 3-point and (b) 4-point bending for a maximum central deflection of 10 mm. Red: auxetic, blue: conventional thin, green: conventional thick.

The conventional thick panel provides the largest energy dissipation, especially under 4-P bending. However, under the same weight conventional sandwich beams absorb more than 4 and 3 times energy than that the auxetic sandwich beams under the 3-point and 4-point tests. Even under the same thickness, conventional sandwich beams still show between 1.5 and 2 times more energy absorption than auxetic ones. When looking at the loss factors, the difference between foams is a lot less defined (Table 2). The auxetic sandwich beams are in this case very close to the loss factor values of the conventional thick sandwich panels subjected to 3-point tests. The loss factors are also slightly increased for 4-point test. The loss factor is defined as the energy dissipated by the specimen as a fraction of the input work: the latter is large for the conventional core thick beams, but smaller for the auxetic sandwich panels, and both show similar loss factors. The conventional foam thin sandwich beams show the highest loss factors, although only 7.2% higher than the auxetic case.

It interesting to observe the behaviour of the loss factors at higher deformations (4-point tests at 10 and 30 mm deflections - Table 3). Increases between 19% to 25% are observed across the 3 types of foam cores when the panels are subjected to 30mm deflections. Albeit slightly, the auxetic foam cores show the highest consistency in terms of results (i.e., minimum error across measurements).

Table 3. Loss factor (in %) for the panels under 4-point tests for 10 and 30 mm

Foam	4-point test (10 mm)	4-point test (30 mm)
Auxetic	5.34 ± 0.35	6.70 ± 0.09
Conventional Thin	5.74 ± 0.16	6.81 ± 0.14
Conventional Thick	5.09 ± 0.14	6.29 ± 0.24

Figure 9 reveals the hysteresis curves during 4-point bending for a maximum central deflection of 30 mm. At larger deformations the loss factor related to the auxetic sandwich beam is larger than that the one of the thick conventional core panels, and very close to the one shown by the conventional foam core thin samples. The auxetic sandwich beam tends to be more compliant at low force levels, but it can sustain higher loading than the conventional sandwich beam with the same thickness under large deformations. Also in this case, it is evident that that negative stiffness behaviour is only present in the conventional thin foam samples, and both the auxetic and the thick conventional foam beams are strain softening.

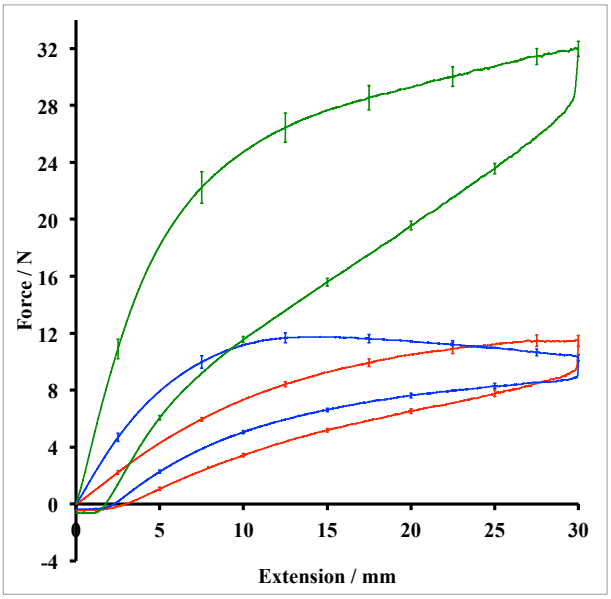

Fig. 9. Hysteresis curves in 4-point bending for a maximum central deflection of 30 mm. Red: auxetic, blue: conventional thin, green: conventional thick.

The loss factors measured under 3P and 4P bending appear to be higher than the values measured under cyclic tension-compression loading on auxetic and conventional foams (between 2.7% and 4.6% [27]). The loss factors measured here are also than the ones observed

in nickel superalloy metal rubber specimens subjected to cyclic quasi-static and dynamic compressive-compressive loading [28][29]. The effect of the composite laminates is likely to be less significant; composite carbon fibre/epoxy prepregs tested with dynamic mechanical analyser setups tend to exhibit bending loss factors (equivalent to Eq. (3)) between 0.5% and 0.6% only [30].

4 Discussions

The core shear modulus extracted from the bending tests of the beams with a conventional thin core is higher than their counterpart measured from the beams with a thick core. Because the specimen have the same 200mm x 80 mm planar surface, it is evident that size effects through-the-thickness play a role. Larger (or thicker) porous samples tend to provide a better indication of the bulk properties of the material, and in that sense the thick beams are more appropriate to follow the hypothesis underlying the application of the ASTM standard [26]. The fact that the shear modulus of the conventional foam measured from the thin sandwich panels is higher than the 'bulk' one may also be related to the higher relative size scale of the thin adhesive layer between the composite face skin and the foam material itself, with a resulting stiffening effect during the bending/shear deformation. The implication of this feature is that the effective shear modulus of this auxetic foam may be even smaller than currently measured. However, the auxetic foam has a density which is 4.3 times higher than the conventional foam, with cell pores around 100 μm [11]. Relative scale size effects existing between the dimensions of the conventional foam cell pores and the overall thickness of the beams are therefore likely to be less important in the case of the NPR foam.

The results related to the shear modulus could be extrapolated for some interesting conclusions related to impact absorption. The shear wave speed in a porous material may be estimated as [31]:

$$w = \sqrt{G/\rho} \tag{4}$$

The energy of travelling waves will tend to be dissipated in the medium according to the modes related to the lowest speed. This is in particular important for helmets and protective equipment to avoid traumatic brain injury (TBI), in which shear waves are the most dangerous for brain tissues [32]. Table 4 clearly shows that auxetic foam has the lowest shear wave speed amongst the ones tested here.

Table 4. Shear wave speeds of the foams considered in this work.

Foam	Shear Modulus (kPa)	Density ($kg.m^{-3}$)	Shear Wave Speed ($m.s^{-1}$)
Auxetic	40.3	129.3 ± 0.5	17.6
Conventional Thin	56.9	30.1 ± 0.1	43.4
Conventional Thick	43.5	30.1 ± 0.1	38.0

To give a benchmark example, expanded polysterene (EPS) liners are currently extensively used in helmets for cyclists and motor biker as shock absorber layers [33]. Table 5 describes the physical properties [34] and shear speed of commercial EPS materials used in helmets applications.

Table 5. Physical properties and shear wave speed of EPSs [34]

EPS	Shear Modulus (kPa)	Density ($kg\ m^{-3}$)	Shear Wave Speed (ms^{-1})
TYPE I	1930 – 2206	14.4 – 18.3	348 – 366
TYPE VIII	2551 – 2827	18.4 – 21.5	363 – 372
TYPE II	3171 – 3447	21.6 – 28.7	347 – 383
TYPE IX	4137 – 4413	28.8 – 35.2	354 – 379

From a comparison between Tables 4 and 5 it is evident how the shear wave speed of the auxetic foam can be up to ~ 22 times lower than the one of EPS foams. Although other design considerations should be also taken when selecting a foam for helmet applications [35], the extremely low shear wave speed, sinclastic curvature and reduced severity index in both frontal and side impacts [20] make auxetic foams quite appealing for crash helmet applications.

Another aspect that this work has highlighted is the quasi-zero stiffness shown by the auxetic sandwich beams under large bending deformations. Negative stiffness has been considered both for controllable large deformations at reduced actuation force [36][37][38], and large damping/energy dissipation [40][41], even with auxetic characteristics [42][43]. Zero stiffness is however another type of anomalous mechanical system with interesting characteristics. Cellular structures with curvature and zero stiffness at medium/large deformations do exhibit hysteresis under cyclic loading (loss factors of ~5% [44], similar to the values found in this work). More importantly, zero stiffness systems have been

mathematically proven to provide a more stable and dissipative answer than negative stiffness ones when subjected to travelling solitons, which could be triggered after impact [45]. The zero stiffness shown by the sandwich laminates with the auxetic core at large bending deformations could therefore be interesting for applications involving sudden impacts with large geometric nonlinear deformations, or potentially for large amplitude vibrations in which zero stiffness isolators are already considered [46].

Conclusions

The paper has described the measurement of the shear modulus and other mechanical properties of auxetic and conventional foams when used as a core in composite sandwich beams subjected to 3-point and 4-point bending loading. The 4-point bending tests have been particular instrumental to understand the behaviour of the foam and the panels under large deformations. The auxetic foams show in general a lower shear modulus compared to their conventional counterpart, but a larger loading capacity (high shear stress) when the beams undergo large deformations. Energy dissipation between the different foams is similar, when considering the loss factors of the hysteretic cycles. The sandwich panels with the auxetic foam core do exhibit interesting zero stiffness behaviour at large deformations, and a general smoother and strain softening behaviour compared to the beams with the conventional cores. The results of the shear properties of these auxetic open cell PU foams produced by thermoforming are used for potential benchmark in energy absorption applications, with some promising design considerations for the production of protective clothing and helmets.

Acknowledgement

FS would like to thank Professor Alessandro Airoldi from the Politecnico of Milano for the useful considerations about shear mechanics. The Authors would also like to than the Reviewers for the very helpful comments and suggestions provided, which have helped to improve the manuscript.

References

[1]. R. S. Lakes. Science 1987, 235, 1038−1040.
[2]. KE Evans, A Alderson. Advanced Materials 2000, 12 (9), 617
[3]. L. J. Gibson, M. F. Ashby, G. S. Schajer, and C. I. Robertson. Proc. Royal Society London 1982, A382, 25-42.
[4]. C.T. Herakovich. J. Composite Materials 1985, 18, 447.
[5]. M Bilski, KW Wojciechowski. Physica Status Solidi (b), 2016, vol. 253 (7), 1318
[6]. K. W. Wojciechowski. Molecular Physics 1987, 61, 1247.
[7]. T Strek, H Jopek and K W Wojciechowski. Smart Materials and Structures 2016, 25(5), 054002
[8]. KW Wojciechowski. Physics Letters A, 1989, vol. 137, pp.60-64
[9]. R Critchley, I Corni, J. A. Wharton, F C. Walsh, R. J. K. Wood, K. R. Stokes, 2013. Physica Status Solid B 250(10), https://doi.org/10.1002/pssb.201248550
[10]. K. Alderson, A. Alderson; N. Ravirala, V. Simkins, P. Davies. Phys. Status Solidi B 2012, 249 (7), 1315.
[11]. M Bianchi, F Scarpa, M Banse, CW Smith. Acta Materialia 2011, 59 (2), 686
[12]. Y. Li, C. Zeng. Polymer 2016, 87, 98−107.
[13]. J. N. Grima, D. Attard, R. Gatt, R. N. A. Cassar. Adv. Eng. Mater. 2009, 11 (7), 533.
[14]. R. Gatt, D. Attard, E. Manicaro, E. Chetcuti, J. N. Grima. Phys. Status Solidi B 2011, 248 (1), 39.
[15]. Y Li, C Zeng. Advanced Materials 2016, 28 (14), 2822-2826.
[16]. A Bezazi, F Scarpa. International Journal of Fatigue 2007, 29(5), 922-930.
[17]. M Bianchi, F Scarpa. Smart Materials and Structures 2013, 22 (8), 084010
[18]. T Allen, T Hewage, C Newton-Mann, W Wang, O Duncan, A Alderson. Physica Status Solidi (b) 2017, 254 (12), 1700596
[19]. O Duncan, T Allen, L Foster, R Gatt, JN Grima, A Alderson. MDPI Proceedings 2018, 2(6), 250
[20]. L Foster, P Peketi, T Allen, T Senior, O Duncan, A Alderson. Applied Sciences 2018, 8(3), 354
[21]. H X Zhu, J F Knott, N J Mills. Journal of the Mechanics and Physics of Solids 1997, 45(3), 319-325.
[22]. A Andersson, S Lundmark, A Magnusson, F H J Maurer. Journal of Applied Polymer Science 2009, 111, 2290-2298

[23]. M S Thompson, I D McCarthy, L Lidgren, L Ryd. ASME Journal of Biomedical Engineering 2003, 123, 732-734.

[24]. ASTM D7250 / D7250M-06 (2012). Standard Practice for Determining Sandwich Beam Flexural and Shear Stiffness. ASTM International, West Conshohocken, PA, www.astm.org

[25]. NMS 128/2 (2011) Hexcel 8552 IM7 Unidirectional Material Specification, National Institute for Aviation Research, Wichita State University, USA.

[26]. G. Caprino, A. Langella. J. Composite Materials 2000, 34, 9, 791.

[27]. M Bianchi, FL Scarpa, CW Smith. Journal of Materials Science 2008, 43(17), 5851

[28]. D Zhang, F Scarpa, Y Ma, K Boba, J Hong, H Lu. Materials Science and Engineering: A 2013, 580, 305

[29]. Y Ma, D Gao, D Zhang, J Hong. Physica Status Solidi (b) 2015, 252(7), 1675

[30]. H Li, Y Niu, C Mu, and B Wen. Shock and Vibration 2017, Article ID 6395739, 13 pages (https://www.hindawi.com/journals/sv/2017/6395739/)

[31]. L J Gibson, M F Ashby. Cellular Solids: structure and property. Cambridge Press, 2nd Edition, Cambridge, 1997.

[32]. E H. Clayton, G M. Genin, P V. Bayly. Journal of The Royal Society Interface 2012, 9, 2899.

[33]. Materials for Bicycle Helmets. (2016). Retrieved 16th April, 2016, from http://www.grantadesign.com/resources/materials/casestudies/helmet.htm

[34]. Physical Properties of Expanded Polystyrene, (EPS). (2007). Retrieved 16th April, 2016, from http://www.northwestfoam.com/fact-specs.htm

[35]. N J Mills, A Gilchrist. International Journal of Impact Engineering 2008, 25, 1087-1101.

[36]. R Lakes. Phil. Mag. Lett. 2012, 92, 226

[37]. S D Guest, E Kebadze, S Pellegrino. J. Mech. Mater. Struct. 2011, 6, 203

[38]. D M Kochmann. Phys. Status Solidi b 2012, 249, 1399

[39]. J N Grima, D Attard, R Caruana-Gauci, R Gatt. Scripta Materialia 2011, 65, 565

[40]. L Dong, R S Lakes. Smart Materials and Structures 2012, 21, 075026

[41]. B M Goldsberry and M R Habermann. Journal of Applied Physics 2018, 123, 091711.

[42]. TAM Hewage, KL Alderson, A Alderson, F Scarpa. Advanced Materials 2016, 28(46), 10323

[43]. B Haghpanah, A Shirazi, L Salari-Sharif, A Guell Izard, LValdevit. Extreme Mechanics Letters 2017, 17, 56

[44]. K Virk, A Monti, T Trehard, M Marsh, K Hazra, K Boba, CDL Remillat, F Scarpa, IR Farrow. Smart Materials and Structures 2013, 22(8), 084014

[45]. F Fraternali, G Carpentieri, A Amendola, RE Skelton, VF Nesterenko. Applied Physics Letters 2014, 105(20), 201903

[46]. A Carrella, M J Brennan,T P Waters. J. Mech. Sci. Technol. 2007, 21, 946